# The dermis contains langerin$^+$ dendritic cells that develop and function independently of epidermal Langerhans cells

Lionel Franz Poulin,[1,2,3] Sandrine Henri,[1,2,3] Béatrice de Bovis,[1,2,3] Elisabeth Devilard,[1,2,3] Adrien Kissenpfennig,[1,2,3] and Bernard Malissen[1,2,3]

[1]Centre d'Immunologie de Marseille-Luminy, Université de la Méditerrannée, Case 906, 13288 Marseille Cedex 9, France
[2]Institut National de la Santé et de la Recherche Médicale, U631, 13288 Marseille Cedex 9, France
[3]Centre National de la Recherche Scientifique, UMR6102, 13288 Marseille Cedex 9, France.

**Langerhans cells (LCs) constitute a subset of dendritic cells (DCs) that express the lectin langerin and that reside in their immature state in epidermis. Paradoxically, in mice permitting diphtheria toxin (DT)–mediated ablation of LCs, epidermal LCs reappeared with kinetics that lagged behind that of their putative progeny found in lymph nodes (LNs). Using bone marrow (BM) chimeras, we showed that a major fraction of the langerin$^+$, skin-derived DCs found in LNs originates from a developmental pathway that is independent from that of epidermal LCs. This pathway, the existence of which was unexpected, originates in the dermis and gives rise to langerin$^+$ dermal DCs (DDCs) that should not be confused with epidermal LCs en route to LNs. It explains that after DT treatment, some langerin$^+$, skin-derived DCs reappear in LNs long before LC-derived DCs. Using CD45 expression and BrdU-labeling kinetics, both LCs and langerin$^+$ DDCs were found to coexist in wild-type mice. Moreover, DT-mediated ablation of epidermal LCs opened otherwise filled niches and permitted repopulation of adult noninflammatory epidermis with BM-derived LCs. Our results stress that the langerin$^+$ DC network is more complex than originally thought and have implications for the development of transcutaneous vaccines and the improvement of humanized mouse models.**

CORRESPONDENCE
Bernard Malissen:
bernardm@ciml.univ-mrs.fr

Abbreviations used: CLN, cutaneous-draining LN; DDC, dermal DC; DT, diphtheria toxin; DTR, DT receptor; EGFP, enhanced GFP; LC, Langerhans cell; MLN, mesenteric LN.

Langerhans cells (LCs) constitute a subset of DCs. In their immature state, they reside in the stratified squamous epidermal layer of the skin and in the mucosal epithelia lining the ocular, oral, and vaginal surfaces. LCs are thought to detect pathogens that penetrate epithelial barriers and, after undergoing a phase of maturation, convey this information via lymphatic vessels to T cells present in LNs (1–3). Recent data suggest that migratory LCs play an indirect role in T cell priming, possibly in carrying over antigens to those DCs that reside throughout their life cycle in LNs (4). These last DCs are denoted as lymphoid tissue–resident DCs to distinguish them from tissue-derived (migratory) DCs (5, 6). Lymphoid tissue–resident DCs are categorized into CD8$\alpha^+$ and CD8$\alpha^-$ subsets and have an "immature" phenotype, which is characterized by low levels of MHC class II (MHCII) and costimulatory molecules. They collect and present antigens in the lymphoid organ itself, and they can respond to activatory signals and mature in situ. In addition to LCs, the skin contains a second type of DC, the dermal DC (DDC). Epidermal LCs and DDCs can migrate to cutaneous-draining LNs (CLNs) under both steady-state and inflammatory conditions, and they constitute the direct precursors of the epidermal LC- and DDC-derived DCs found in CLNs, respectively. These two types of skin-derived DCs express a "mature" phenotype, which is characterized by a CD11c$^{\text{inter to high}}$, MHCII$^{\text{high}}$ phenotype and high levels of costimulatory molecules. Tissue-derived DCs are also found in LNs that do not drain skin territories, such as mesenteric LNs (MLNs), and likely represent the progeny of interstitial DCs found in the parenchyma of nonlymphoid tissues.

Langerin (CD207) is a C-type lectin that is expressed in LCs (7, 8). To track LCs in vivo

L. Poulin and S. Henri contributed equally to this paper.
A. Kissenpfennig's present address is Infection and Immunity Group, Centre for Cancer Research and Cell Biology, School of Biomedical Sciences, Queen's University, Belfast, Northern Ireland.
The online version of this article contains supplemental material.

and distinguish them from DDCs, *Lang-EGFP* mice that express an enhanced GFP (EGFP) under the control of the *langerin* gene were engineered (9). Although langerin expression is down-regulated upon LC maturation, LCs still retain detectable levels of langerin once they reach CLNs (10), and langerin$^+$ DCs could be readily identified in the T cell zone of steady-state CLNs (9). However, langerin alone is not a reliable marker to identify LC-derived DCs outside the skin because most CD8$\alpha^+$ DCs present in CLNs, MLNs, and the spleen express langerin, albeit at lower levels than LCs (9). Therefore, lymphoid tissue–resident DCs differentiating from blood precursors can express langerin without having to reside first within epithelia. Because they do not drain skin territories, the spleen and MLNs contain only langerin$^{low}$ CD8$\alpha^+$ DCs, whereas CLNs contain both lymphoid tissue–resident, langerin$^{low}$, CD8$\alpha^+$ DCs and skin-derived, langerin$^+$, CD8$\alpha^{-\text{ to low}}$ DCs.

Epidermal LCs renew throughout life from local cells that seed the skin around birth (11, 12). Importantly, the cells ensuring epidermal LC renewal are radiation resistant, and after lethal irradiation and BM transplantation, epidermal LCs and their derivatives found in CLNs remain of host origin throughout life (12). In contrast, all other DC subtypes, including most DDCs, are radiosensitive and replaced by donor-derived cells (13). Experiments based on parabiotic mice have suggested that, akin to epidermal LCs, some lymphoid tissue–resident DCs are replaced by locally derived, long-lived precursors, and thus do not depend on the continuous extravasation and differentiation of blood precursors (14–16). However, this view has been recently challenged (17), and in steady-state conditions, lymphoid tissue–resident DC homeostasis likely results from three processes that consist of constant replenishment by DC precursors from blood, limited in situ divisions, and cell death.

Knock-in mice expressing a diphtheria toxin (DT) receptor (DTR) cDNA under the control of the *langerin* gene (*Lang-DTR-EGFP* mice) were used to study the dynamics of LCs in vivo (9, 18). Expression of the DTR-EGFP fusion protein conferred DT sensitivity to langerin$^+$ DCs, whereas other DC subsets remained resistant to DT treatment. DT treatment resulted in no sign of skin inflammation, and 24 h after a single injection of DT the whole population of epidermal LCs was eliminated (9, 18). 2 wk after DT treatment, sparse patches of LCs were observed in the epidermis, and it is only 8 wk after DT treatment that epidermal LC reconstitution was close to completion. According to currently accepted views, langerin$^+$, CD11c$^{inter\ to\ high}$, MHCII$^{high}$ DCs present in steady-state CLNs constitute terminally differentiated cells that are endowed with a short half-life and that are continuously replaced by migratory LCs. After DT treatment, the kinetics of reappearance of the langerin$^+$, CD11c$^{inter\ to\ high}$, MHCII$^{high}$ DCs found in CLNs was thus expected to lag behind that of epidermal LCs. Unexpectedly, the langerin$^+$, CD11c$^{inter\ to\ high}$, MHCII$^{high}$ DC cells found in CLNs were reconstituted over 7 d (9), a kinetics much faster than that of epidermal LCs and similar to that of the DT-sensitive, lymphoid tissue–resident, langerin$^{low}$ CD8$\alpha^+$ DCs that are found in CLNs and are continuously renewed from blood-precursors. There is currently no explanation for this unanticipated observation. In this study, we demonstrate that a major fraction of the langerin$^+$, skin-derived DCs found in steady-state CLNs follows a developmental pathway that is both independent from and proceeds at a faster pace than that of epidermal LCs and their derivatives.

## RESULTS

### Dual origin of the langerin$^+$ DCs found in CLNs

Considering that the expression of the *Lang-DTR-EGFP* allele results in dimmer EGFP fluorescence than that of the *Lang-EGFP* allele, and that a single copy of the *Lang-DTR-EGFP* allele renders langerin$^+$ DCs sensitive to DT (9), we systematically used mice with a *Lang-EGFP/Lang-DTR-EGFP* genotype to track LCs in vivo and facilitate depletion monitoring. For the sake of brevity, *Lang-EGFP/Lang-DTR-EGFP* mice are subsequently denoted as *Lang-DTR-EGFP* mice. To revisit the origin of the langerin$^+$, CD11c$^{inter\ to\ high}$, MHCII$^{high}$ DCs found in steady-state CLNs, C57BL/6 mice expressing the CD45.1 allele (B6 [CD45.1]) were lethally irradiated and reconstituted with BM cells isolated from *Lang-DTR-EGFP* mice expressing the CD45.2 allele. These chimeras, called *Lang-DTR-EGFP* → B6 (CD45.1) chimeras, were analyzed 8 wk after transplantation. At that time, >99% of blood B cells were of donor origin (Fig. S1, available at http://www.jem.org/cgi/content/full/jem.20071724/DC1), and the radiosensitive DC subsets were made of BM-derived DCs only (Fig. S2 and Fig. S3). Owing to their radioresistance (12), all the epidermal LCs found in *Lang-DTR-EGFP* → B6 (CD45.1) chimera 8 wk after BM transplantation were of host (CD45.1$^+$) origin and expressed langerin, but no EGFP (Fig. 1 A), confirming that in the absence of major skin injury there is no input of donor-derived cells to the pool of epidermal LCs. In contrast, LCs from epidermal sheets of *Lang-DTR-EGFP* control mice expressed both langerin and EGFP (Fig. 1 A). The tissue-derived (CD11c$^{inter\ to\ high}$, MHCII$^{high}$) DCs found in CLNs of *Lang-DTR-EGFP* → B6 (CD45.1) chimera segregated into a langerin$^-$ and langerin$^+$ fraction and, consistent with a recent study (13), >90% of the DDC-derived DCs were of donor origin (Fig. 1 B). Provided LCs constitute the only reservoir of the langerin$^+$, CD11c$^{inter\ to\ high}$, MHCII$^{high}$ DCs found in the CLNs of *Lang-DTR-EGFP* → B6 (CD45.1) chimeras, these last cells should constitute a homogeneous CD45.1$^+$, EGFP$^-$ population. However, they segregated into a CD45.1$^+$, EGFP$^-$ subset, which likely derives from the migration of radioresistant, B6 (CD45.1)-derived LCs (Fig. 1 A), and into a donor-derived (CD45.2$^+$, EGFP$^+$) subset, the existence of which was unexpected and the immediate precursors of which do not reside in the epidermis. Therefore, the langerin$^+$, CD11c$^{inter\ to\ high}$, MHCII$^{high}$ DCs found in CLNs do not derive exclusively from migratory epidermal LCs.

The unexpected subset of donor-derived, langerin$^+$ DCs found in steady-state CLNs of *Lang-DTR-EGFP* → B6 (CD45.1) chimeras does not constitute a minor component

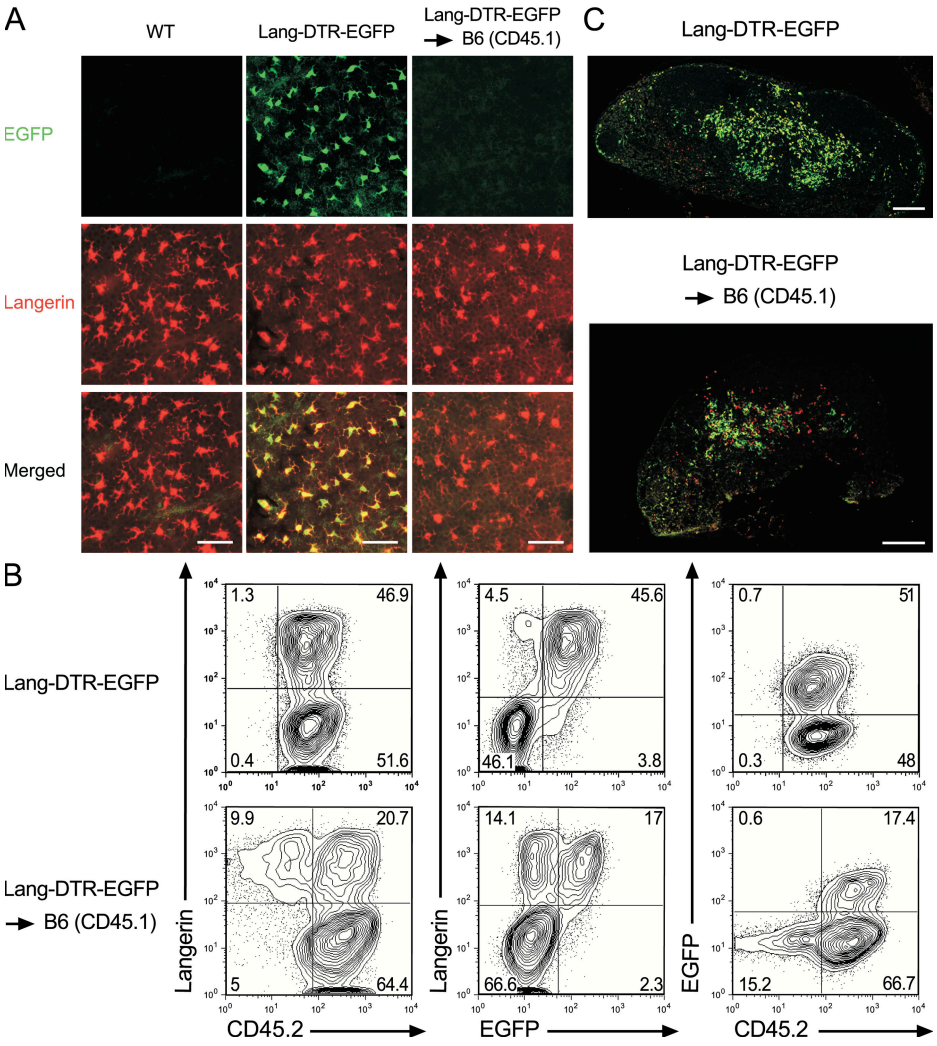


**Figure 1. Two developmental pathways give rise to langerin⁺ skin-derived DCs found in CLNs.** (A) Staining of epidermal sheets from *Lang-DTR-EGFP* → B6 (CD45.1) chimeras, wild-type (WT), and *Lang-DTR-EGFP* mice with an anti-langerin antibody (red). As expected, the langerin⁺ cells found in the epidermis of *Lang-DTR-EGFP* mice differ from those of WT mice and of *Lang-DTR-EGFP* → B6 (CD45.1) chimeras in that they express EGFP. Genotypes are indicated for each column and markers on the left. Results are representative of at least 10 mice of each genotype. (B) Tissue-derived DCs found in CLNs were defined on the basis of their CD11c$^{inter\ to\ high}$ MHCII$^{high}$ phenotype (Fig. S2), and analyzed for the expression of langerin versus CD45.2, langerin versus EGFP, and EGFP versus CD45.2. Contour plots from *Lang-DTR-EGFP* CLNs are also included for comparison. The percentages indicated for each window correspond to the percentage of cells among CD11c$^{inter\ to\ high}$, MHCII$^{high}$ DCs. Results are representative of at least five experiments. (C) Staining of a CLN section from a *Lang-DTR-EGFP* → B6 (CD45.1) chimera with an anti-langerin antibody (red) shows that host-derived (EGFP⁻ langerin⁺) LCs colocalize with donor-derived (EGFP⁺ langerin⁺) LCs. A stained section from *Lang-DTR-EGFP* mice is shown for comparison. Bars: (A) 50 μm; (C) 200 μm.

of the langerin⁺, CD11c$^{inter\ to\ high}$, MHCII$^{high}$ DCs. For instance, the donor- and host-derived langerin⁺ DCs found in the CLNs of *Lang-DTR-EGFP* → B6 (CD45.1) chimeras ($n$ = 13) represented 59.7 ± 11.0% and 36.3 ± 9.9% of the langerin⁺, CD11c$^{inter\ to\ high}$, MHCII$^{high}$ DCs, respectively. As shown in Fig. 3 B, donor- and host-derived langerin⁺ DCs were also observed in the CLNs of chimeras resulting from transfer of B6 (CD45.1) BM cells into lethally irradiated *Lang-DTR-EGFP* recipient mice. In this reverse combination, denoted as B6 (CD45.1) → *Lang-DTR-EGFP* chimeras, the donor- and host-derived langerin⁺ DCs found in CLNs represented 69.4 ± 12.5% and 23.6 ± 8.4% of the langerin⁺, CD11c$^{inter\ to\ high}$, MHCII$^{high}$ DCs, respectively ($n$ = 4). Therefore, the donor-derived langerin⁺ DCs found in steady-state CLNs of both type of chimeras are two- to three-times more abundant than LC-derived DCs. It should be stressed that such substantial numbers of donor-derived langerin⁺ DCs arise in the presence of an epidermis that is entirely filled with host-derived LCs. This finding suggests that two parallel developmental pathways generate the langerin⁺, CD11c$^{inter\ to\ high}$, MHCII$^{high}$ DCs found in steady-state CLNs.

### Developmental independence of the two langerin+ DC subsets

To support the developmental independence of the two langerin+, CD11c$^{inter\ to\ high}$, MHCII$^{high}$ DC subsets identified in steady-state CLNs of BM chimeras, B6 (CD45.1) → *Lang-DTR-EGFP* chimeras were used to specifically ablate the host-derived, DT-sensitive, epidermal LCs and their progeny found in CLNs. Provided that donor-derived langerin+ DCs develop independently of host-derived LCs, DT treatment of B6 (CD45.1) → *Lang-DTR-EGFP* chimeras should have no effect on them and allow the analysis of this novel subset in isolation. In contrast to the situation observed in *CD11c-DTR-EGFP* mice (19), repeated injections of DT into *Lang-DTR-EGFP* mice did not result in any deleterious effect (9). Therefore, B6 (CD45.1) → *Lang-DTR-EGFP* chimeras were treated with 3 injections of DT 1 wk apart and analyzed at various time points after the third injection. 1 d after the last DT injection, epidermal sheets of B6 (CD45.1) → *Lang-DTR-EGFP* chimeras did not contain any LCs, as detected using EGFP expression and antibodies directed against langerin (Fig. 2 A). Ear explants from B6 (CD45.1) → *Lang-DTR-EGFP* chimeras that had received 3 injections of DT were prepared 1 day after the last injection and cultured in medium containing the CCL21 chemokine (20). CD11c+, MHCII+ DCs migrating out of the ear explants were analyzed using langerin versus CD45.2 dot plots and epidermal

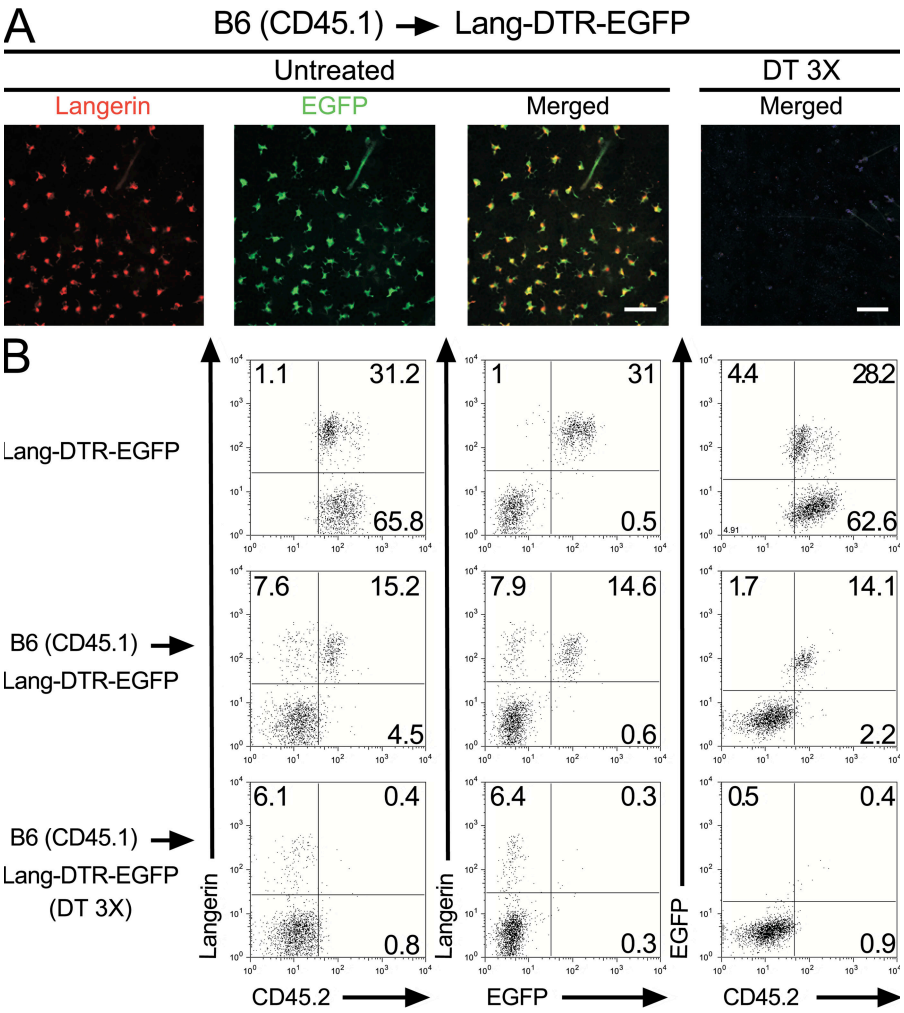


**Figure 2. Donor-derived langerin+ DCs are found in skin explants.** (A) Confocal microscopic analysis of epidermal sheets from B6 (CD45.1) → *Lang-DTR-EGFP* chimera that were left untreated (untreated) or had received 3 injections of DT (DT 3 X) a week apart were analyzed 1 d after the last DT injection. Staining with anti-langerin antibody (red) revealed the presence of langerin+ EGFP+ LCs in untreated sheets and their complete absence 1 d after the last DT injection. Bars: (untreated panel) 50 μm; (DT-treated panel) 300 μm. Results are representative of at least two experiments. (B) Ear explants from B6 (CD45.1) → *Lang-DTR-EGFP* chimera that had received 3 injections of DT (DT 3 X) were prepared 1 d after the last injection and cultured in the presence of CCL21. CD11c+ MHCII+ cells migrating out of the ear explants were analyzed by using langerin-CD45.2, langerin-EGFP, and EGFP-CD45.2 plots. Ear explants from untreated B6 (CD45.1) → *Lang-DTR-EGFP* chimera and *Lang-DTR-EGFP* mice were also included for comparison. The percentages indicated for each window corresponds to the percentage of cells among CD11c+, MHCII+ cells. Results are representative of at least two experiments.

LC-derived DCs were found to be absent (Fig. 2 B). Therefore, congruent with histological analysis (Fig. 2 A), and with previous data (9, 18), DT treatment completely eliminated the pool of host-derived, epidermal LCs (CD45.2$^+$, EGFP$^+$). Langerin$^+$ DCs with a donor-derived (CD45.2$^-$, EGFP$^-$) phenotype were still found among the cells that migrated out of the ear of DT-treated B6 (CD45.1) → *Lang-DTR-EGFP* chimeras (Fig. 2 B). In contrast, both donor- and host-derived langerin$^+$ DCs migrated out from the ear of untreated B6 (CD45.1) → *Lang-DTR-EGFP* chimeras (Fig. 2 B). Considering that the epidermis of DT-treated B6 (CD45.1) → *Lang-DTR-EGFP* chimeras contains no detectable langerin$^+$ cells (Fig. 2 A), it is likely that the population of langerin$^+$, donor-derived DCs that migrated out of the ear explants originated from the dermis. Microscopic examination of section of ear from DT-treated B6 (CD45.1) → *Lang-DTR-EGFP* chimeras 1 day after the last DT injection, confirmed that langerin$^+$ EGFP$^-$ cells with DC morphology can be readily identified in the dermis (Fig. 3 A and not depicted). Therefore, the lack of host-derived, epidermal LCs in DT-treated B6 (CD45.1) → *Lang-DTR-EGFP* chimeras 1 day after the last DT injection allowed the unambiguous identification of a population of donor-derived, langerin$^+$ DCs that reside in the dermis. Importantly, this experimental model prevents these unexpected langerin$^+$ DCs to be mistakenly confounded with epidermal LCs in transit to CLNs. For the sake of brevity, the novel population of radiosensitive langerin$^+$ DCs that reside in the dermis will be denoted as langerin$^+$ DDCs. This subset represents approximately a third of the langerin$^+$ DCs capable of being mobilized from ear

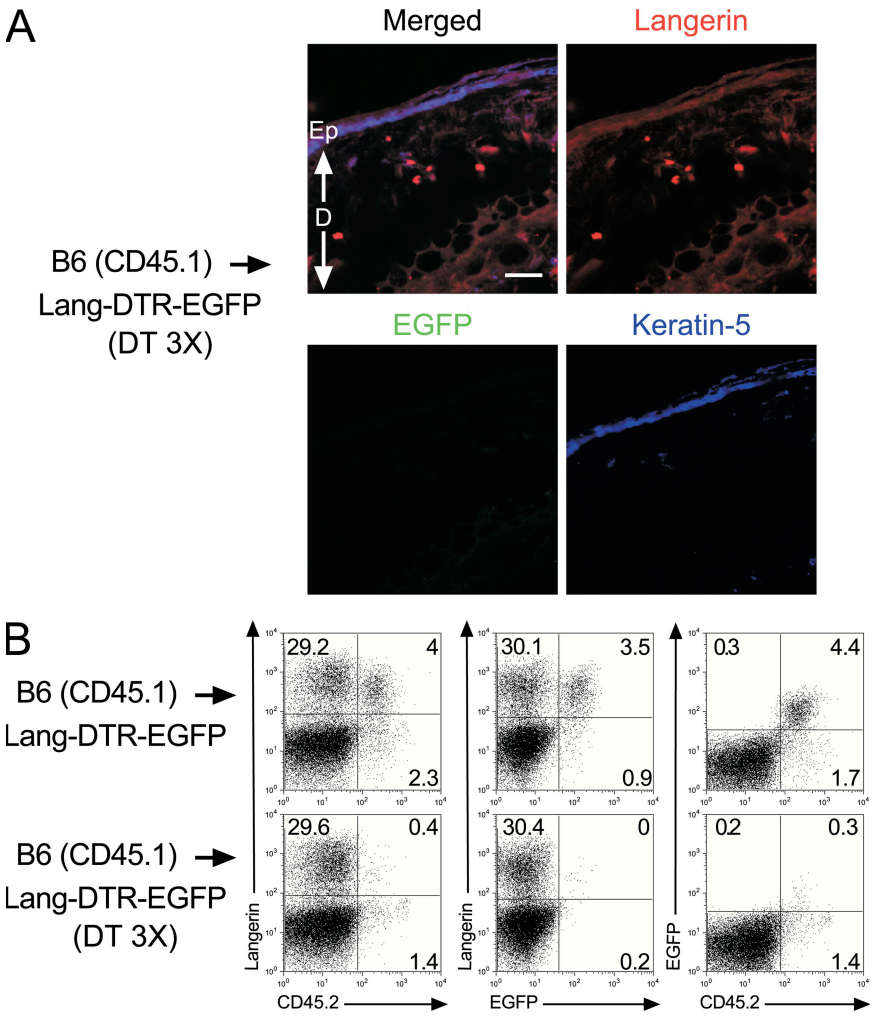


**Figure 3. Donor-derived langerin$^+$ DCs are located in the skin dermis.** (A) Staining of sections of ear from B6 (CD45.1) → *Lang-DTR-EGFP* chimera that had received 3 injections of DT and were prepared 1 d after the last injection were stained with anti-langerin (red) and anti-keratin 5 (blue) antibodies. Staining with the anti-keratin 5 antibody allowed visualization of the epidermis. Donor-derived, langerin$^+$ DCs (EGFP$^-$, langerin$^+$) are exclusively found in the dermis. Bar, 30 μm. Ep, epidermis; D, dermis. Results are representative of at least two experiments. (B) CLNs of DT-treated B6 (CD45.1) → *Lang-DTR-EGFP* chimera were collected 1 d after the last DT injection. Tissue-derived (CD11c$^{inter\ to\ high}$, MHCII$^{high}$) DCs were analyzed as described in the legend of Fig. 1 for the expression of langerin-CD45.2, langerin-EGFP, and EGFP-CD45.2. The percentage indicated for each window corresponds to the percentage of cells among CD11c$^{inter\ to\ high}$, MHCII$^{high}$ DCs. Results are representative of at least 4 experiments.

explants upon CCL21 treatment (Fig. 2 B). Therefore, based on langerin expression, DDCs can be subdivided into a langerin$^+$ and a langerin$^-$ subset.

Consistent with the lack of LCs in the skin epidermis of DT-treated B6 (CD45.1) → *Lang-DTR-EGFP* chimeras, the corresponding CLNs contained no LC-derived (CD45.2$^+$, EGFP$^+$) DCs (Fig. 3 B and not depicted). In contrast, the same CLNs contained langerin$^+$ DCs that showed a tissue-derived phenotype (CD11c$^{\text{inter to high}}$, MHCII$^{\text{high}}$) and originated from the transplanted BM cells (CD45.2$^-$, EGFP$^-$, Fig. 3 B). Altogether, the data obtained using both types of BM chimeras support the view that the langerin$^+$, CD11c$^{\text{inter to high}}$, MHCII$^{\text{high}}$ DCs found in steady-state CLNs have a dual origin. The coincidence that exists in DT-treated B6 (CD45.1) → *Lang-DTR-EGFP* chimeras between the presence of donor-derived, langerin$^+$ DDCs in the dermis and of donor-derived, langerin$^+$, CD11c$^{\text{inter to high}}$, MHCII$^{\text{high}}$ DCs in the CLNs suggests that a precursor-product relationship links them. Consistent with that view, donor-derived, langerin$^+$, CD11c$^{\text{inter to high}}$, MHCII$^{\text{high}}$ DCs were absent from secondary lymphoid organs (MLNs and spleen) that do not drain cutaneous territories (Fig. S2).

### Kinetics of replacement of langerin$^+$ DCs after DT ablation

If the langerin$^+$ DDCs identified in the two types of BM chimeras constitute the main reservoir of the langerin$^+$, CD11c$^{\text{inter to high}}$, MHCII$^{\text{high}}$ DCs found in CLNs, their kinetics of restoration after DT treatment should be faster than for their putative progeny found in CLNs. To assess the kinetics of reappearance of langerin$^+$ DDCs after DT treatment, ear explants from DT-treated *Lang-DTR-EGFP* → B6 (CD45.1) chimeras were prepared at various time points after the last DT injection and cultured in the presence of CCL21 (Fig. 4). CD11c$^+$, MHCII$^+$ cells migrating out of the ear explants were analyzed using langerin-EGFP dot plots and the percentage of langerin$^+$ DDCs (langerin$^+$, EGFP$^+$) determined (Fig. 4). The use of *Lang-DTR-EGFP* → B6 (CD45.1) chimeras instead of *Lang-DTR-EGFP* mice allows us to readily distinguish langerin$^+$ DDCs from LCs. 24 h after the last DT injection, no langerin$^+$ DDCs can be observed among the CD11c$^+$, MHCII$^+$ cells that migrated out of the ear (Fig. 4). Langerin$^+$ DDCs reappeared around day 4 and their pool was gradually restored over the next 14 d (Fig. 4). Confocal microscopic analysis of a section of ear from *Lang-DTR-EGFP* → B6 (CD45.1) chimeras 14 d after the last DT injection confirmed langerin$^+$ DDC restoration (Fig. 4). Parallel analysis of the langerin$^+$ DDC-derived DCs present in the CLNs of DT-treated *Lang-DTR-EGFP* → B6 chimeras showed that they reappeared with kinetics that are slightly protracted relative to those of the langerin$^+$ DDCs (Fig. 4), an observation consistent with their postulated precursor–product relationship.

The aforementioned data suggest that langerin$^+$ DDCs constitute the reservoir of the langerin$^+$, CD11c$^{\text{inter to high}}$, MHCII$^{\text{high}}$ DCs that rapidly reappeared in CLNs of *Lang-DTR-EGFP* → B6 (CD45.1) chimeras after interruption of DT treatment. To support this putative precursor–product relationship, small pieces of spleen, CLNs, or MLNs from B6 (CD45.1) mice were transplanted under the renal capsule of B6 (CD45.2) mice. This approach has recently been used to show that DC subsets present in the spleen are replenished over a 10–14-d period (17). Consistent with that last finding, 3 wk after transplantation, most of the DCs found in the grafts were of B6 (CD45.2) origin (Fig. S5). Analysis of

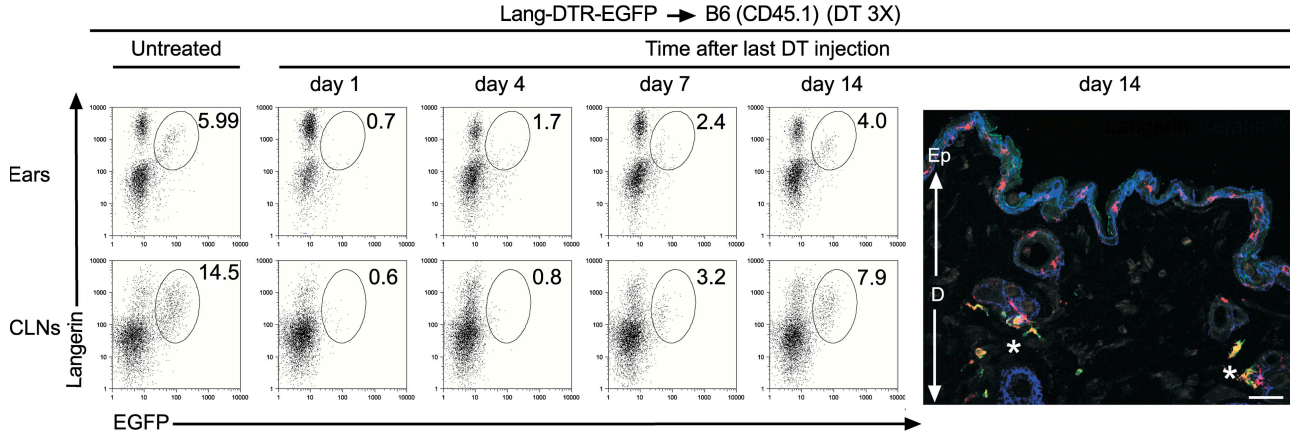


**Figure 4. Kinetics of reappearance of donor-derived langerin$^+$ DCs after DT ablation.** Ear explants and CLNs from *Lang-DTR-EGFP* → B6 (CD45.1) chimeras that had received 3 injections of DT 1 wk apart were prepared at the specified time points after the last DT treatment. For ears, analysis was performed on cells migrating out of CCL21-treated ear explants. Gated DCs (ears, CD11c$^+$ MHCII$^+$; CLNs, CD11c$^{\text{inter to high}}$ MHCII$^{\text{high}}$) were analyzed using langerin-EGFP plots. A window corresponding to the langerin$^+$ EGFP$^+$ subset is shown. The percentage indicated for this window corresponds to the percentage of donor-derived, langerin$^+$, EGFP$^+$ cells within the DC gates specified above. Also shown is a confocal microscopic analysis of a section of ear from a DT-treated *Lang-DTR-EGFP* → B6 (CD45.1) chimera 14 d after the last DT treatment. Staining with anti-langerin (red) and anti-keratin 5 (blue), revealed that donor-derived (EGFP$^+$), langerin$^+$ DCs are located exclusively in the dermis, whereas host-derived (EGFP$^-$), langerin$^+$ DCs are found in the epidermis. Some donor-derived, langerin$^+$ DDCs (marked with a star) are found adjacent to hair follicles. Results are representative of at least two experiments. Ep, epidermis; D, dermis. Bar, 30 μm.

CD11c-MHCII dot plots corresponding to the CD45.2$^+$ DCs present in the grafts showed that they contained blood-derived, lymphoid-resident DC subsets only. Because they were totally deprived of tissue-derived (CD11c$^{\text{inter to high}}$, MHCII$^{\text{high}}$) DCs, the CD11c-MHCII profiles of the CLN and MLN grafts resembled those of transplanted pieces of spleen or of unmanipulated spleen (Fig. S5). Therefore, akin to LCs, langerin$^+$ DDCs presumably reach CLN via afferent lymphatic vessels.

### The BrdU labeling kinetics of langerin$^+$ DDCs resemble that of langerin$^-$ DDCs

To examine the turnover of the langerin$^+$ DDCs and compare it to that of LCs and langerin$^-$ DDCs, *Lang-DTR-EGFP* → B6 (CD45.1) chimeras were continuously exposed to BrdU for a week, and ear explants were prepared. DCs migrating out of ear explants cultured in the presence of CCL21 were gated on CD11c$^+$, MHCII$^+$ DCs and analyzed using langerin-CD45.2 dot plot. We found that 7.7% of LCs (langerin$^+$, CD45.2$^-$) and 49% of langerin$^+$ DDCs (langerin$^+$, CD45.2$^+$) were labeled with BrdU within 7 d (Fig. 5). The slow BrdU labeling kinetics of LCs is consistent with previous data (12, 21), and starkly contrasts with the faster BrdU labeling observed for langerin$^+$ DDCs. Interestingly, langerin$^-$ DDCs exhibit a BrdU labeling rate that is of the same order (52.1%) as the one observed for langerin$^+$ DDCs. Therefore, half of the langerin$^+$ DDCs or their direct precursors have divided within the 7 d during which BrdU was administered. Analysis of langerin$^+$ DDCs for the expression of Ki-67, a nuclear antigen of which the expression reflects an active proliferative state, showed that most langerin$^+$ DDCs were Ki67$^-$ (unpublished data). Regardless of the exact nature of the proliferative progenitors (local langerin$^-$ precursors or continuously extravasating blood precursors) that replenish the pool of langerin$^+$ DDCs, our data emphasize that the BrdU labeling kinetics of langerin$^+$ DDCs resembles that of langerin$^-$ DDCs and is markedly distinct from that of epidermal LCs.

### LCs and langerin$^+$ DDCs coexist in wild-type mice

Analysis of LC-derived DCs and langerin$^+$ DDC-derived DCs present in CLNs of BM chimeras showed that they are CD8α$^{-\text{ to low}}$ and that they express rather similar levels of CD11c, CD205, and CD207 molecules (Figs. S2 and S3). The high levels of MHCII, CD40, and CD86 molecules they express are typical of tissue-derived DCs (Figs. S2 and S4). LC-derived DCs and langerin$^+$ DDC-derived DCs also showed an overlapping anatomical distribution within the inner paracortex of CLNs (Fig. 1 C). Extraction of langerin$^+$ DDCs from the skin of *Lang-DTR-EGFP* → B6 (CD45.1) chimeras further revealed that >90% of them are CD11c$^+$ and MHCII$^+$ (unpublished data).

Based on a wealth of surface markers normally used to discriminate DC subsets, we failed to distinguish langerin$^+$ DDCs and their derivatives from LCs and their derivatives. However, on langerin-CD45.2 dot plots, the langerin$^+$ DCs that migrated out from the ear of untreated *Lang-DTR-EGFP* mice segregated into CD45.2$^{\text{high}}$ and CD45.2$^{\text{inter}}$ subsets (Fig. 2 B). Parallel analysis of B6 (CD45.1) → *Lang-DTR-EGFP* chimeras

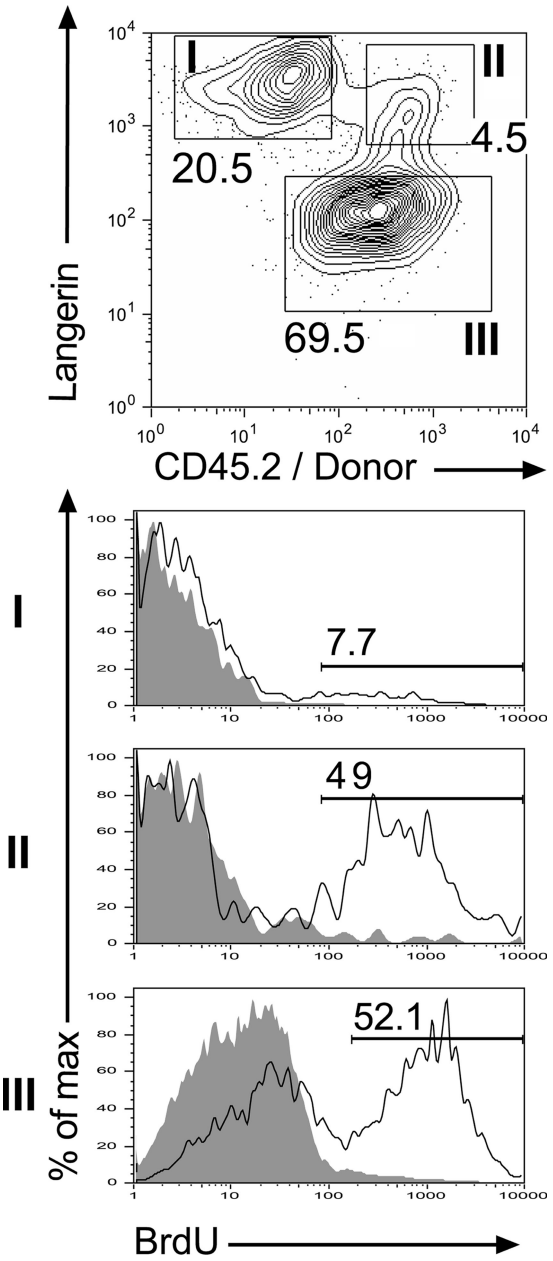


**Figure 5. BrdU incorporation of host- and donor-derived langerin$^+$ DCs found in the skin.** *Lang-DTR-EGFP* → B6 (CD45.1) chimeras were exposed to BrdU for 1 wk, and ear explants were prepared. DCs migrating out of the ear explants were gated on CD11c$^+$, MHCII$^+$ cells and analyzed. Three subsets can be distinguished using langerin versus CD45.2 dot plots: host-derived LCs (subset I: langerin$^+$, CD45.2$^-$, EGFP$^-$), donor-derived, langerin$^+$ DDCs (subset II: langerin$^+$, CD45.2$^+$, EGFP$^+$), and donor-derived, langerin$^-$ DDCs (subset III: langerin$^-$, CD45.2$^+$, EGFP$^-$). Histograms show BrdU incorporation for each subset. Gray-filled histograms correspond to control staining profile of mice that received no BrdU. Percentages of BrdU$^+$ cells are indicated. Results are representative of at least two experiments.

showed that the CD45.2$^{high}$ subset is missing from langerin$^+$ DCs that migrated out from CCL-21 ear explant and replaced by langerin$^+$, CD45.2$^-$ donor DCs (Fig. 2 B). Moreover, the langerin$^+$, CD45.2$^{inter}$ subset left in B6 (CD45.1) → *Lang-DTR-EGFP* chimeras disappeared after DT treatment (Fig. 2 B). This suggests that the langerin$^+$ DDCs and LCs migrating out of ear explants are CD45.2$^{high}$ and CD45.2$^{inter}$, respectively. Therefore, by combining such differential expression of CD45.2 with the markedly distinct BrdU labeling kinetics observed for LCs and langerin$^+$ DDCs (Fig. 2 B and Fig. 5), we reasoned that it should be possible to validate the existence of two distinct langerin$^+$ DC subsets in the skin of wild-type mice. Accordingly, wild-type B6 (CD45.2) mice were left untreated or exposed to continuous BrdU labeling for 1 wk. Ear explants were prepared, and the CD11c$^+$, MHCII$^+$ DCs migrating out of the explant analyzed using langerin-CD45.2 contour plots. Two discrete subsets of langerin$^+$ DCs could readily be identified on the basis of CD45.2 levels (Fig. 6). In support of the hints provided by Fig. 2 B, the CD45.2$^{inter}$, langerin$^+$ subset showed BrdU labeling kinetics that resembled those of LCs, whereas the CD45.2$^{high}$, langerin$^+$ subset showed a rate of BrdU labeling comparable to langerin$^+$ DDCs (compare Figs. 5 and 6). Therefore, two subsets of langerin$^+$ DCs can be discriminated in the skin of wild-type mice on the basis of the expression of CD45.2 and of BrdU labeling kinetics. LCs correspond to CD45.2$^{inter}$ cells with slow BrdU labeling kinetics, whereas langerin$^+$ DDCs correspond to CD45.2$^{high}$ cells with faster BrdU labeling kinetics. Although the two discrete clusters of CD45.2$^{high}$ and CD45.2$^{inter}$ langerin$^+$ DCs tend to merge in the CLNs, the LC versus langerin$^+$ DDC distinction still held true when cells belonging to both extremities of the CD45.2 distribution were analyzed (unpublished data). Therefore, both LCs and langerin$^+$ DDCs coexist in wild-type mice.

### Colonization of emptied noninflammatory epidermis by donor-derived LCs

Under steady-state conditions or upon minor skin injuries, renewal of the pool of epidermal LCs does not require any input from blood-borne, BM-derived cells. However, once a strong local inflammation is reached, e.g., through high-dose UV exposure, the local LC-generative compartment is destroyed (12). The emptied epidermis is then slowly recolonized by LCs that derive from blood-borne precursors (22). In contrast to high-dose UV exposure that induces a strong inflammation, DT treatment of B6 (CD45.1) → *Lang-DTR-EGFP* chimeras provides the unique opportunity to ablate epidermal LCs in the absence of detectable inflammation (9, 18), and to determine whether an LC-emptied, noninflammatory adult epidermis is still competent to attract donor-derived cells capable of reconstituting the pool of epidermal LCs.

Epidermal sheets of ears from DT-treated B6 (CD45.1) → *Lang-DTR-EGFP* chimeras were prepared and analyzed at various time points after the last DT injection. As shown in Figs. 2, 3, and 7, host-derived (EGFP$^+$) epidermal LCs were absent at all the time points analyzed (from 24 h to 7 wk).

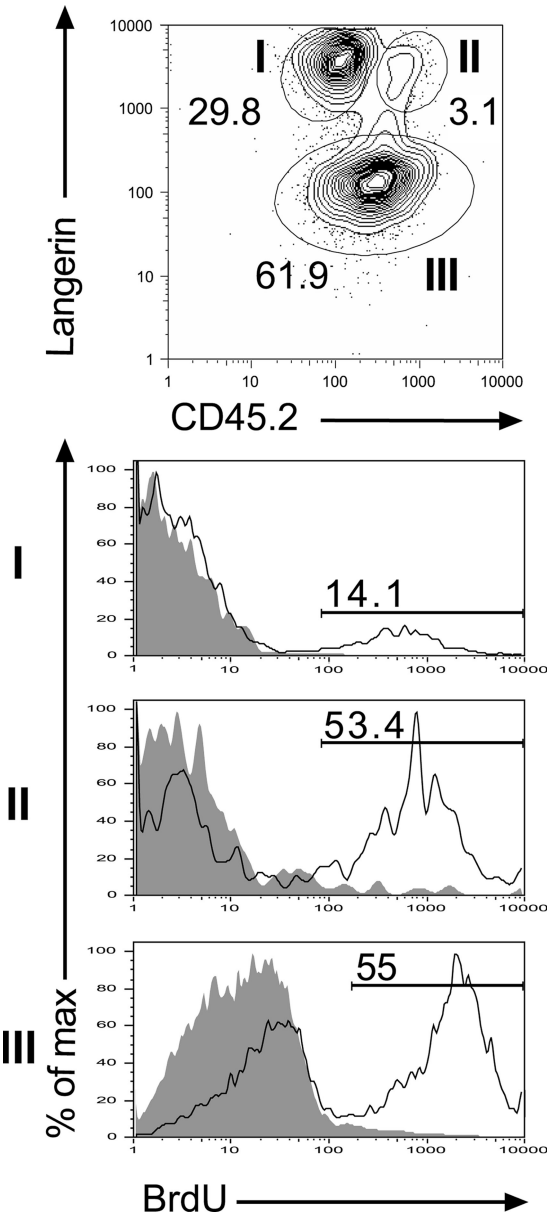


**Figure 6. Wild-type langerin$^+$ DDCs express higher levels of CD45.2 than wild-type epidermal LCs.** Wild-type C57BL/6 (CD45.2$^+$) mice were left untreated or exposed to BrdU for 1 wk, and ear explants were prepared and cultured in the presence of CCL21. The MHCII$^+$, CD11c$^+$ DCs migrating out of the ear explants were analyzed using langerin-CD45.2 plots. Two discrete subsets can be readily discriminated among langerin$^+$ DCs according to the levels of CD45.2 they express. Subset I corresponds to LCs and expresses intermediate levels of CD45.2, whereas subset II corresponds to langerin$^+$ DDCs and expresses high levels of CD45.2. Subset III corresponds to langerin$^-$ DDCs. Histograms show BrdU incorporation for each subset. Gray-filled histograms correspond to control staining profile of mice that received no BrdU. Percentages of BrdU$^+$ cells are indicated. Results are representative of at least two experiments.

Therefore, DT treatment of B6 (CD45.1) → *Lang-DTR-EGFP* chimeras completely eliminated the local, host-derived, LC-generative compartment, allowing us to analyze whether

an LC-free, noninflammatory, adult epidermis has the capacity to be repopulated with BM-derived LCs. As shown in Fig. 7 A, the emptied epidermis of DT-treated B6 (CD45.1) → *Lang-DTR-EGFP* chimeras was, indeed, recolonized with donor-derived (langerin$^+$, EGFP$^-$) LCs. Interestingly, repopulation of the adult epidermis occurred very slowly, and at 1 wk after the last DT injection, only sparse foci of langerin$^+$ cells with a DC morphology were observed (Fig. 7 A). 4 wk after the last DT injection, langerin$^+$ cells still showed a patchy distribution, suggesting that the whole ear epidermis is repopulated by only a few donor-derived cells, the clonal progeny of which start to merge only at later time points (Fig. 7 A). Microscopic analysis of a skin section of a DT-treated B6 (CD45.1) → *Lang-DTR-EGFP* chimera 7 wk after the last DT injection confirmed the presence of langerin$^+$ cells within the epidermis (Fig. 7 A). Therefore, the use of DT-treated B6 (CD45.1) → *Lang-DTR-EGFP* chimeras instead of DT-treated *Lang-DTR-EGFP* mice (9, 18), permitted us to establish that an LC-emptied, noninflammatory epidermis can be reconstituted through BM-derived precursors rather than through host-derived, langerin$^-$ (DT-unsensitive) LC precursors. Interestingly, the slow kinetics of reappearance of the epidermal LCs observed in B6 (CD45.1) → *Lang-DTR-EGFP* chimera after DT treatment resembles that noted under strong inflammatory conditions (22). These two observations are thus in marked contrast with the fast kinetics of reappearance noted for langerin$^+$ DDCs and their derivatives (Fig. 4), suggesting that the epidermal environment might lower the rate of LC division.

## DISCUSSION

Two subsets of langerin$^+$ DCs are currently distinguished in steady-state CLNs (9, 23). The main subset represents ∼90% of the langerin$^+$ cells and shows a tissue-derived phenotype (CD11c$^{\text{inter to high}}$, MHCII$^{\text{high}}$) matching that expected for LC-derived DCs. The second subset represents ∼10% of the langerin$^+$ fraction and corresponds to lymphoid tissue–resident, langerin$^{\text{low}}$, CD8α$^+$ DCs. In this study, we showed that the langerin$^+$, CD11c$^{\text{inter to high}}$, MHCII$^{\text{high}}$ DC subset originates from two independent developmental pathways that coexist in steady-state conditions. The first pathway corresponds to the paradigmatic pathway established for radioresistant epidermal LCs and for their derivatives found in CLNs. The second pathway originates from langerin$^+$ CD11c$^+$ MHCII$^+$ DCs that reside in the dermis. These langerin$^+$ DDCs are radiosensitive and should not be confused with migratory epidermal LCs that coexist in the dermis of steady-state mice and are en route to the CLNs. After migrating through lymphatic vessels, both LC-derived DCs and langerin$^+$ DDC-derived DCs colocalize into the T-cell zones of the CLNs. In DT-treated B6 (CD45.1) → *Lang-DTR-EGFP* chimeras, langerin$^+$ DDC-derived DCs can be observed in CLNs even at the earliest time points after DT treatment, a period characterized by the absence of epidermal LCs. Therefore, langerin$^+$ DDCs do not appear to develop through a default pathway that operates only when precursor cells are prevented from reaching LC-replete epidermis. Using combined CD45.2 expression and BrdU labeling kinetics, we further showed that epidermal LCs and langerin$^+$ DDCs are present in the skin of wild-type mice, and thus do not constitute artifacts resulting from the use of BM chimeras. Therefore, langerin alone is not a reliable marker to identify LC outside the epidermis and the skin-derived, langerin$^+$, CD8α$^{-\text{ to low}}$ DCs proper to CLNs include two subsets that markedly differ in their developmental origin (Fig. S6).

DT-mediated ablation of the radioresistant epidermal LCs present in B6 (CD45.1) → *Lang-DTR-EGFP* chimeras opened otherwise filled niches in the absence of detectable inflammation. This maneuver allowed the seeding of the epidermis with incoming donor-derived LCs. Seeding occurred in a focal manner, suggesting that the pool of reconstituted epidermal LCs stems from the progeny of only a few cells. In the case of adult steady-state epidermis, it has been questioned whether local LC renewal is achieved through LC precursors with stem-cell properties or through division of differentiated LCs. The observation that the LC clusters developing around the first langerin$^+$ incoming cells expand centrifugally with age suggests that differentiated LCs self-duplicate within the epidermis, although proliferation and differentiation in the dermis and a subsequent focused migration into the epidermis cannot be excluded. In support of the first view, it should be noted that after acute injuries, liver regeneration occurs through proliferation of hepatocytes and without obvious participation of stem cells (24).

When parabiotic mice are separated after DC "equilibration," lymphoid tissue–resident DCs present in the spleen and originating from the separated partner reach background levels by 10–14 d, and are replaced by blood-borne precursors (17). A similar trend, corresponding to a 5–7-d half-life, is also observed for the tissue-derived (MHC$^{\text{high}}$) DCs found in CLNs and originating from the separated partner (17). Although this compartment was analyzed without segregating it into the derivatives of LCs, of langerin$^+$ DDCs, and of langerin$^-$ DDCs, the bulk of it also reached background levels by 10–14 d (17). After DT ablation, we found that the pool of langerin$^+$ DDCs is almost completely reconstituted over a 14-d period. It is thus tempting to speculate that blood precursors are continuously recruited into noninflammatory dermis to replace langerin$^+$ DDCs en route to the CLNs. In the chimeric mice used in this study, donor-derived langerin$^+$ DDCs represented approximately a third of the langerin$^+$ DCs capable of being mobilized from ear explants (Fig. 2 B). In the corresponding CLNs, the donor-derived langerin$^+$ CD11c$^{\text{inter to high}}$, MHCII$^{\text{high}}$ DCs that are expected to derive from langerin$^+$ DDCs comprised from 60% (*Lang-DTR-EGFP* → B6 [CD45.1] chimeras; Fig. 1) to 70% (B6 [CD45.1] → *Lang-DTR-EGFP* chimeras; Fig. 3) of the langerin$^+$ CD8α$^{-\text{ to low}}$ DCs. The distortion that exists in the ratio of LCs/langerin$^+$ DDCs in CCL21-treated ear explants and of LC-derived DCs/langerin$^+$ DDC-derived DCs in CLNs suggests that CCL21 treatment might favor the migration of LCs. Alternatively, a fraction of the donor-derived, langerin$^+$

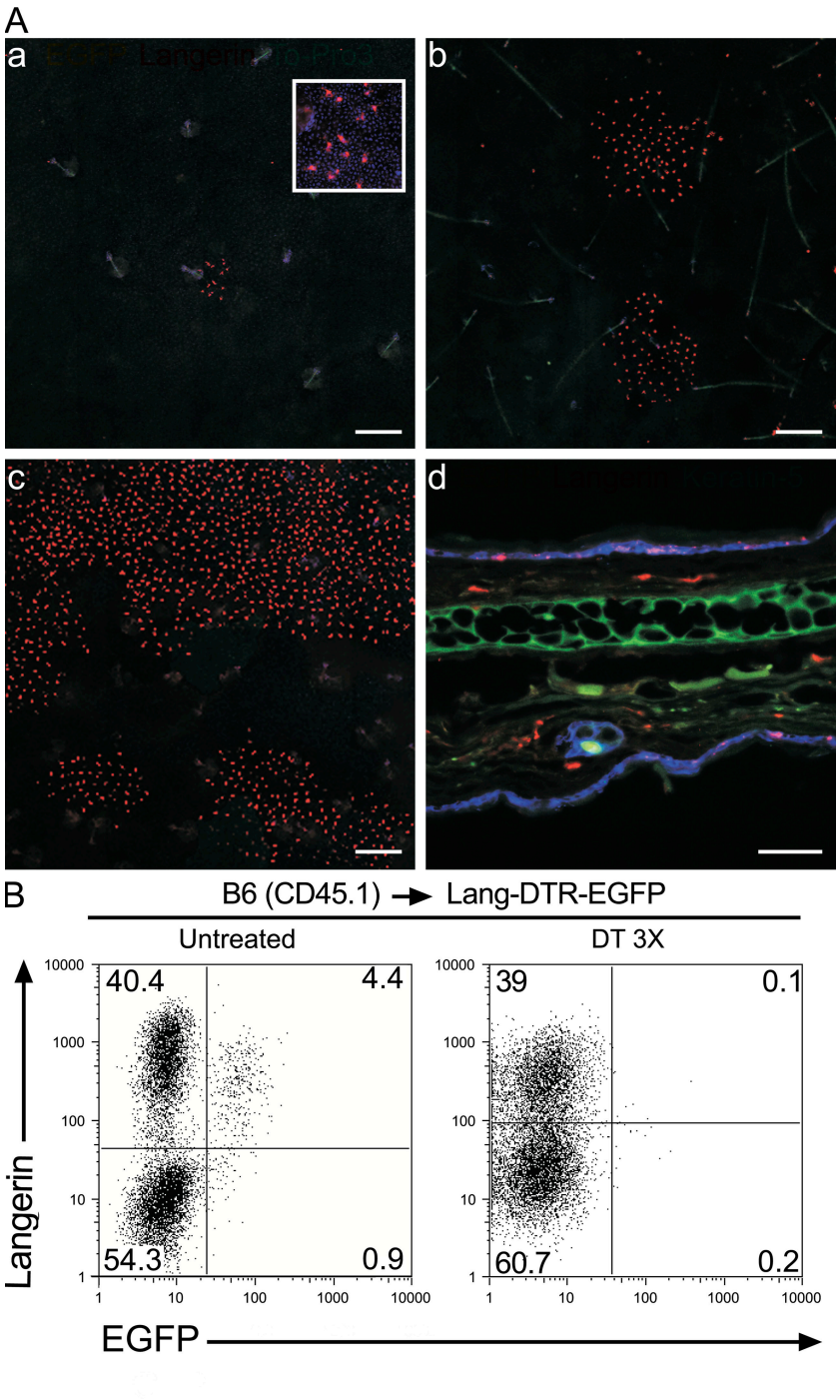


**Figure 7. Donor-derived LCs colonize emptied epidermal niches.** B6 (CD45.1) → *Lang-DTR-EGFP* chimeras that had received 3 injections of DT 1 wk apart were analyzed at various time points after the last injection. (A) Epidermal sheets 1 (a), 4 (b), and 7 wk (c) after the last DT injection were stained with anti-langerin antibody (red) and ToPro3 blue. Rare patches of donor-derived LCs (langerin$^+$ EGFP$^-$) were found 1 wk after the last injection (arrow). An enlarged view (206.8 × 206.8 µm) of one of these patches is shown in the top right corner of a. d corresponds to a section of an ear from a DT-treated B6 (CD45.1) → *Lang-DTR-EGFP* chimera 7 wk after the last DT injection costained with anti-langerin (red) and –keratin 5 (blue) antibodies. Donor-derived LCs are found in both the dermis and epidermis. Bars: (a–c) 200 µm; (d) 50 µm. Results are representative of at least two experiments with two to three mice per experiment. Ep, epidermis; D, dermis. (B) Analysis of tissue-derived (CD11c$^{\text{inter to high}}$, MHCII$^{\text{high}}$) DCs present in the CLNs from untreated and DT-treated B6 (CD45.1) → *Lang-DTR-EGFP* chimera. In the case of the DT-treated mice, CLNs were analyzed 7 wk after the last DT-injection. Dot plots show langerin-EGFP distribution. Consistent with the results shown in A, 7 wk after the last DT injection, the CLNs of DT-treated B6 (CD45.1) → *Lang-DTR-EGFP* chimera are deprived of host-derived LCs and contain an abundant population of donor-derived LCs. Results are representative of at least two experiments.

$CD11c^{inter\ to\ high}$, $MHCII^{high}$ DCs found in the CLNs of the chimeras can originate from precursors that are recruited directly to the CLNs from the blood. It has been shown that an inflammed skin can project its chemokine profile to the high endothelial venules of CLNs, and thereby exert some "remote control" on the composition of the leukocytes that home to the CLNs from the blood (25). Likewise, in non-inflammatory skin, inductive signals might also be projected to CLNs via afferent lymphatics and allow the differentiation of blood-derived precursors into $langerin^+$ $CD11c^{inter\ to\ high}$, $MHCII^{high}$ DCs. If proven, the existence of such inductive mechanisms will question the categorization of DCs into lymphoid tissue–resident and tissue-derived subsets because they will confer a bona fide tissue-derived phenotype ($MHCII^{high}$, $CD40^+$, $CD86^+$; Figs. S2 and S4) to DCs that never resided in the skin. However, as demonstrated in a companion paper (26), through the use of mice that lack the chemokine receptor CCR7, most of the $langerin^+$, $CD8\alpha^{-\ to\ low}$ DCs likely reach CLNs through skin afferent lymphatics, and thus constitute the direct progeny of LCs and of $langerin^+$ DDCs (Fig. S6).

The exact function of LCs remains enigmatic. For instance, in a mouse model of HSV infection, LCs were found dispensable for the generation of viral-specific effector T cells (for review see [2]), and conflicting results were reached as to the role of LCs in triggering hapten-specific T cell effectors through skin immunization (9, 18, 27). Efforts aiming at determining the relative contribution of epidermal LCs and DDCs in the presentation of skin-delivered pathogen antigens have generally relied on the use of BM chimeras that use recipients expressing the H-2 $K^{bm1}$ gene (28). This natural variant gene arose by gene conversion from the H-2 $K^b$ gene, and its product is incapable of presenting a peptide derived from HSV and recognized by the gBT-I T-cell antigen receptor. Accordingly, the whole population of $langerin^+$, skin-derived DCs present in CLNs of H-2 $K^b \rightarrow$ H-2 $K^{bm1}$ chimeras was inferred to express H-2 $K^{bm1}$, and thus to be unable to present the HSV-derived peptide. This conclusion should, however, be revised on the basis of this study because $langerin^+$ DDC-derived DCs present in H-2 $K^b \rightarrow$ H-2 $K^{bm1}$ chimeras would be expected to express H-2 $K^b$, and thus contribute to trigger gBT-I T cells in addition to $langerin^-$ DDC-derived DCs. Further experiments aiming at probing the role of $langerin^+$ DCs and relying on H-2 $K^b \rightarrow$ H-2 $K^{bm1}$ chimeras should thus take into consideration the existence of two $langerin^+$, skin-derived DC subsets that markedly differ in their origin and radioresistance.

Finally, it remains to determine whether some functional specialization exists among the two types of $langerin^+$ skin-derived DC subsets described in this study. For instance, the TGF-β1 rich epidermal environment might specifically lower the capacity of LCs to present antigen in an immunogenic form. Provided it extends to humans, the LCs versus $langerin^+$ DDCs dichotomy described in this study might also be important to take into consideration during HIV-1 infection. For instance, the langerin molecules that decorate the surface of human $langerin^+$ DCs endow such cells with unique antigen uptake and processing capacities (29, 30). Therefore, the rapidly renewing $langerin^+$ DDC subset described in this study might provide the host with a second line of defense to react to pathogens that naturally infect the dermis or that reach it via a disrupted epithelial barrier. Mouse strains lacking T, B, and NK cells support engraftment and differentiation of human hematopoietic stem cells. Such humanized mice have allowed us to model issues such as intervention in HIV-1 infections and hematopoietic and immune system gene therapy. However, as recently outlined by Manz (31), these mice present major limitations and need further improvements to make them appropriate for human immunology research. Particularly relevant to this data, their epidermis remains populated with radioresistant LCs of mouse origin. We have shown that DT-mediated ablation of the host-derived, radioresistant epidermal LCs present in B6 (CD45.1) → *Lang-DTR-EGFP* chimeras allows the replenishment of the epidermis with donor-derived LCs. Applying a similar strategy to humanized mouse models carrying a *Lang-DTR-EGFP* allele should thus facilitate the colonization of the mouse epidermis by epidermal LCs of human origin and contribute to improving such models.

## MATERIALS AND METHODS

**Mice.** C57BL/6 female mice that express the CD45.1 (B6 [CD45.1]) or CD45.2 (B6 [CD45.2]) allele of CD45 were purchased from Charles River Laboratories. *Langerin-EGFP* and *Langerin-DTR-EGFP* mice have been previously described (9) and crossed onto the B6 background for at least 10 generations. Mice were housed under specific pathogen-free conditions and handled in accordance with French and European directives (DDSV des Bouches du Rhône).

**Transplantation of BM cells.** 7–8-wk-old B6 (CD45.1) mice were lethally irradiated with 2 doses of 475 rads each, 5 h apart, and then injected i.v. with BM cells ($2 \times 10^6$) obtained from adult $CD45.2^+$ *Lang-DTR-EGFP-DTR* mice. In the case of B6 (CD45.1) → *Lang-DTR-EGFP* chimera, proper engraftment was obtained by irradiating the recipient mice with 2 doses of 550 rads each, 5 h apart, and i.v. injection with $5 \times 10^6$ BM cells isolated from B6 (CD45.1) mice. 7–8 wk after reconstitution, the level of blood chimerism was determined. Chimeras were kept on antibiotic-containing water (0.2% Bactrim; Roche) during the whole experiment.

**Preparation and staining of epidermal sheets.** Epidermal sheets were prepared as previously described (20), and their integrity was systematically assessed by counterstaining with the nuclear stain ToPro3.

**DC isolation.** DCs were isolated from lymphoid organs, as previously described (32). In brief, the organs were first cut in small pieces and incubated with a mixture of type II collagenase (Worthington Biochemical) and of DNase (Sigma-Aldrich). Light density cells were purified by centrifugation on a Nycoprep solution (density = 1.068). DCs were isolated from cultured ear skin explants, as previously described (20).

**Flow cytometry.** Before staining, cells were preincubated on ice for at least 10 min with the 2.4 G2 mAb to block Fc receptors. Multiparameter FACS analysis was performed using an LSR or a FACSCanto system (BD Biosciences). FACS data were analyzed using FlowJo software (Tree Star, Inc.). For each experiment, control mice (B6 [CD45.2], B6 [CD45.1], and *Lang-DTR-EGFP* mice) were included to define the proper gates. Autofluorescent

cells were gated out by using the FL3 (LSR) or AmCyan (Canto) channel. In a few experiments, the fixation procedure used to detect the surface and intracellular content of langerin resulted in some EGFP leak and DCs with the lowest EGFP intensity scored in the langerin$^+$ EGFP$^-$ quadrant of langerin-EGFP plots. The langerin versus CD45.2 staining is not prone to such a caveat, and it gives the correct relative percentages of cells. For instance, in Fig. 1 B, correction of the langerin-EGFP plots for such a leak (4.5%) resulted in percentages of donor- and host-derived EGFP$^+$ cells that are congruent with those based on langerin-CD45.2 staining.

**Antibodies.** CD11c (HL3), CD8α (53–6.7), CD40 (HM40-3), MHCII (M5/114 or AF6-120.1), CD86 (GL1), CD45.2 (104), CD45.1 (A20), and B220 (RA3-6B2) antibodies were all purchased from BD Biosciences, except for CD205 (CL89145; Cedarlane Laboratories), CD115 (AFS98; eBioscience), and the anti-langerin antibody (929F3; Dendritics).

**Histology, immunostaining, and confocal microscopy.** LNs and ears were fixed by incubating them on ice for 1–2 h in PBS containing 3.2% PFA. To preserve cell morphology, organs were briefly washed in PBS and transferred to a 35% sucrose solution for 24–48 h. Fixed tissues were frozen in Tissue-Tec OCT on dry ice and stored at −80°C until further processing. Cryosections (20 μm thick) were rehydrated in PBS and permeabilized by placing them in PBS with 0.5% saponin for 10 min. After washing in PBS, nonspecific antibody-binding sites were blocked with PBS, 1% FCS, 2% normal goat serum, and 2% BSA. Cryosections were stained overnight at 4°C with the primary antibody. After a wash in PBS, the secondary antibody was added for 2 h at room temperature. Finally, cryosections were washed successively in PBS and water and mounted in ProLong Gold antifade reagent (Invitrogen). Rabbit anti-EGFP antibody (clone TP401; Torrey Pines Biolabs) and rat anti-langerin antibody (clone 929F3; Dendritics) were revealed using an Alexa Fluor 488 goat anti–rabbit IgG and an Alexa Fluor 546 goat anti–rat IgG, respectively (Invitrogen). Rat anti-langerin antibody and rabbit anti-keratin 5 antibody (clone AF138; Eurogentec) were revealed using an Alexa Fluor 546 goat anti–rat IgG and an Alexa Fluor 647 goat anti–rabbit IgG, respectively. Images were acquired on a confocal microscope (LSM 510; Carl Zeiss, Inc.).

**In vivo depletion of LCs.** For systemic in vivo depletion of langerin$^+$ DCs, mice were injected i.p. with 1 μg DT (Servibio). Mice were analyzed at different time points after the last DT injection.

**BrdU labeling in vivo and cell cycle analyses.** Mice were injected i.p. with 1.5 mg BrdU (Sigma-Aldrich) to ensure its immediate availability, and their drinking water was supplemented for 1 wk with 0.8 mg/ml of BrdU and 2% glucose and changed daily. DCs collected from ear explants were stained first for surface markers and then permeabilized for BrdU staining (BrdU labeling Flow kit; BD Biosciences) and langerin staining.

**Renal capsule grafting.** Spleen pieces were grafted under the renal capsule according to an online procedure (http://mammary.nih.gov/tools/mousework/cunha001/index.html). This protocol was recently used to determine the origin of the DCs found in the spleen (17), and extended in this study to total or to pieces of CLNs and MLNs. To avoid necrosis of the center of the graft before revascularization, the largest dimension of the grafted piece did not exceed 2 mm.

**Online supplemental material.** Fig. S1 shows the extent of chimerism 8 wk after BM transplantation. Fig. S2 shows that DC subsets found in CLNs, MLNs, and spleen of chimeric mice have an expected developmental origin and anatomical distribution. Fig. S3 compares CD205 and CD8α expression on LC-derived DCs and langerin$^+$ DDC-derived DCs from chimeric and *Lang-DTR-EGFP* mice. Fig. S4 shows that both host- and donor-derived DCs from steady-state CLNs of chimeric mice display a mature phenotype. Fig. S5 shows host DC development in grafted pieces of secondary lymphoid organs. Fig. S6 shows a model of the origin of the three langerin$^+$ DC subsets found in steady-state CLNs. The online version of this article is available at http://www.jem.org/cgi/content/full/jem.20071724/DC1.

We thank M. Malissen, L. Leserman, A.M. Schmitt-Verhulst, M. Mingueneau, D. Kaiserlian, B. Dubois, and Jean Davoust for discussion, and Pierre Perrin for maintaining the mouse colony.

This work was supported by Centre National de la Recherche Scientifique, Institut National de la Santé et de la Recherche Médicale (PNR Dermatologie), Agence Nationale pour la Recherche (ANR; Project DC in vivo), European Communities (MUGEN Network of Excellence), L'Association pour la recherche sur le Cancer, L'Association Française contre les Myopathies, and La Fondation pour la Recherche Médicale (FRM). L.F. Poulin was supported by a fellowship from FRM and E. Devilard by ANR.

The authors declare that they have no competing financial interests.

**Submitted: 13 August 2007**
**Accepted: 19 October 2007**

## REFERENCES

1. Steinman, R.M., and M.C. Nussenzweig. 2002. Avoiding horror autotoxicus: the importance of dendritic cells in peripheral T cell tolerance. *Proc. Natl. Acad. Sci. USA*. 99:351–358.
2. Villadangos, J.A., and P. Schnorrer. 2007. Intrinsic and cooperative antigen-presenting functions of dendritic-cell subsets in vivo. *Nat. Rev. Immunol.* 7:543–555.
3. Larregina, A.T., and L.D. Falo. 2005. Changing paradigms in cutaneous immunology: adapting with dendritic cells. *J. Invest. Dermatol.* 124:1–12.
4. Carbone, F.R., G.T. Belz, and W.R. Heath. 2004. Transfer of antigen between migrating and lymph node-resident DCs in peripheral T-cell tolerance and immunity. *Trends Immunol.* 25:655–658.
5. Shortman, K., and S.H. Naik. 2007. Steady-state and inflammatory dendritic-cell development. *Nat. Rev. Immunol.* 7:19–30.
6. Wu, L., and Y.J. Liu. 2007. Development of dendritic-cell lineages. *Immunity*. 26:741–750.
7. Valladeau, J., O. Ravel, C. Dezutter-Dambuyant, K. Moore, M. Kleijmeer, Y. Liu, V. Duvert-Frances, C. Vincent, D. Schmitt, J. Davoust, et al. 2000. Langerin, a novel C-type lectin specific to Langerhans cells, is an endocytic receptor that induces the formation of Birbeck granules. *Immunity*. 12:71–81.
8. Kissenpfennig, A., S. Ait-Yahia, V. Clair-Moninot, H. Stossel, E. Badell, Y. Bordat, J.L. Pooley, T. Lang, E. Prina, I. Coste, et al. 2005. Disruption of the langerin/CD207 gene abolishes Birbeck granules without a marked loss of Langerhans cell function. *Mol. Cell. Biol.* 25:88–99.
9. Kissenpfennig, A., S. Henri, B. Dubois, C. Laplace-Builhe, P. Perrin, N. Romani, C.H. Tripp, P. Douillard, L. Leserman, D. Kaiserlian, et al. 2005. Dynamics and function of Langerhans cells in vivo dermal dendritic cells colonize lymph node areas distinct from slower migrating Langerhans cells. *Immunity*. 22:643–654.
10. Stoitzner, P., S. Holzmann, A.D. McLellan, L. Ivarsson, H. Stossel, M. Kapp, U. Kammerer, P. Douillard, E. Kampgen, F. Koch, et al. 2003. Visualization and characterization of migratory Langerhans cells in murine skin and lymph nodes by antibodies against Langerin/CD207. *J. Invest. Dermatol.* 120:266–274.
11. Tripp, C.H., S. Chang-Rodriguez, P. Stoitzner, S. Holzmann, H. Stossel, P. Douillard, S. Saeland, F. Koch, A. Elbe-Burger, and N. Romani. 2004. Ontogeny of Langerin/CD207 expression in the epidermis of mice. *J. Invest. Dermatol.* 122:670–672.
12. Merad, M., M.G. Manz, H. Karsunky, A. Wagers, W. Peters, I. Charo, I.L. Weissman, J.G. Cyster, and E.G. Engleman. 2002. Langerhans cells renew in the skin throughout life under steady-state conditions. *Nat. Immunol.* 3:1135–1141.
13. Bogunovic, M., F. Ginhoux, A. Wagers, M. Loubeau, L.M. Isola, L. Lubrano, V. Najfeld, R.G. Phelps, C. Grosskreutz, E. Scigliano, et al. 2006. Identification of a radio-resistant and cycling dermal dendritic cell population in mice and men. *J. Exp. Med.* 203:2627–2638.
14. Zhang, M., H. Tang, Z. Guo, H. An, X. Zhu, W. Song, J. Guo, X. Huang, T. Chen, J. Wang, and X. Cao. 2004. Splenic stroma drives mature dendritic cells to differentiate into regulatory dendritic cells. *Nat. Immunol.* 5:1124–1133.

15. Kabashima, K., T.A. Banks, K.M. Ansel, T.T. Lu, C.F. Ware, and J.G. Cyster. 2005. Intrinsic lymphotoxin-beta receptor requirement for homeostasis of lymphoid tissue dendritic cells. *Immunity*. 22:439–450.
16. Naik, S.H., D. Metcalf, A. van Nieuwenhuijze, I. Wicks, L. Wu, M. O'Keeffe, and K. Shortman. 2006. Intrasplenic steady-state dendritic cell precursors that are distinct from monocytes. *Nat. Immunol.* 7:663–671.
17. Liu, K., C. Waskow, X. Liu, K. Yao, J. Hoh, and M. Nussenzweig. 2007. Origin of dendritic cells in peripheral lymphoid organs of mice. *Nat. Immunol.* 8:578–583.
18. Bennett, C.L., E. van Rijn, S. Jung, K. Inaba, R.M. Steinman, M.L. Kapsenberg, and B.E. Clausen. 2005. Inducible ablation of mouse Langerhans cells diminishes but fails to abrogate contact hypersensitivity. *J. Cell Biol.* 169:569–576.
19. Jung, S., D. Unutmaz, P. Wong, G. Sano, K. De los Santos, T. Sparwasser, S. Wu, S. Vuthoori, K. Ko, F. Zavala, et al. 2002. In vivo depletion of CD11c(+) dendritic cells abrogates priming of CD8(+) T cells by exogenous cell-associated antigens. *Immunity*. 17:211–220.
20. Henri, S., D. Vremec, A. Kamath, J. Waithman, S. Williams, C. Benoist, K. Burnham, S. Saeland, E. Handman, and K. Shortman. 2001. The dendritic cell populations of mouse lymph nodes. *J. Immunol.* 167:741–748.
21. Kamath, A.T., S. Henri, F. Battye, D.F. Tough, and K. Shortman. 2002. Developmental kinetics and lifespan of dendritic cells in mouse lymphoid organs. *Blood*. 100:1734–1741.
22. Ginhoux, F., F. Tacke, V. Angeli, M. Bogunovic, M. Loubeau, X.M. Dai, E.R. Stanley, G.J. Randolph, and M. Merad. 2006. Langerhans cells arise from monocytes in vivo. *Nat. Immunol.* 7:265–273.
23. Douillard, P., P. Stoitzner, C.H. Tripp, V. Clair-Moninot, S. Ait-Yahia, A.D. McLellan, A. Eggert, N. Romani, and S. Saeland. 2005. Mouse Lymphoid Tissue Contains Distinct Subsets of Langerin/CD207 Dendritic Cells, Only One of Which Represents Epidermal-Derived Langerhans Cells. *J. Invest. Dermatol.* 125:983–994.
24. Blanpain, C., V. Horsley, and E. Fuchs. 2007. Epithelial stem cells: turning over new leaves. *Cell*. 128:445–458.
25. Palframan, R.T., S. Jung, G. Cheng, W. Weninger, Y. Luo, M. Dorf, D.R. Littman, B.J. Rollins, H. Zweerink, A. Rot, and U.H. von Andrian. 2001. Inflammatory chemokine transport and presentation in HEV: a remote control mechanism for monocyte recruitment to lymph nodes in inflamed tissues. *J. Exp. Med.* 194:1361–1373.
26. Ginhoux, F., M.P. Collin, M. Bogunovic, M. Abel, M. LeBoeuf, J. Helft, J. Ochando, A. Kissenpfennig, B. Malissen, M. Grisotto, H. Snoeck, G. Randolph, and M. Merad. 2007. Blood-derived dermal langerin$^+$ dendritic cells survey the skin in the steady state. *J. Exp. Med.* 204:3133–3146.
27. Kaplan, D.H., M.C. Jenison, S. Saeland, W.D. Shlomchik, and M.J. Shlomchik. 2005. Epidermal langerhans cell-deficient mice develop enhanced contact hypersensitivity. *Immunity*. 23:611–620.
28. Allan, R.S., C.M. Smith, G.T. Belz, A.L. van Lint, L.M. Wakim, W.R. Heath, and F.R. Carbone. 2003. Epidermal viral immunity induced by CD8alpha+ dendritic cells but not by Langerhans cells. *Science*. 301:1925–1928.
29. de Witte, L., A. Nabatov, M. Pion, D. Fluitsma, M.A. de Jong, T. de Gruijl, V. Piguet, Y. van Kooyk, and T.B. Geijtenbeek. 2007. Langerin is a natural barrier to HIV-1 transmission by Langerhans cells. *Nat. Med.* 13:367–371.
30. Hladik, F., P. Sakchalathorn, L. Ballweber, G. Lentz, M. Fialkow, D. Eschenbach, and M.J. McElrath. 2007. Initial events in establishing vaginal entry and infection by human immunodeficiency virus type-1. *Immunity*. 26:257–270.
31. Manz, M.G. 2007. Human-hemato-lymphoid-system mice: opportunities and challenges. *Immunity*. 26:537–541.
32. Vremec, D., J. Pooley, H. Hochrein, L. Wu, and K. Shortman. 2000. CD4 and CD8 expression by dendritic cell subtypes in mouse thymus and spleen. *J. Immunol.* 164:2978–2986.